Short Note

(Z)-3-(Dicyanomethylene)-4-((5-fluoro-3,3-dimethyl-1-(3-phenylpropyl)-3*H*-indol-1-ium-2-yl)methylene)-2-(((*E*)-5-fluoro-3,3-dimethyl-1-(3-phenylpropyl)indolin-2-ylidene)methyl)cyclobut-1-en-1-olate

Stefanie Casa [1] ![ORCID], **Guliz Ersoy Ozmen** [1] **and Maged Henary** [1,2,*] ![ORCID]

[1] Department of Chemistry, Petit Science Center, Georgia State University, 100 Piedmont Avenue SE, Atlanta, GA 30303, USA

[2] Center for Diagnostics and Therapeutics, Petit Science Center, Georgia State University, 100 Piedmont Avenue SE, Atlanta, GA 30303, USA

* Correspondence: mhenary1@gsu.edu

Abstract: Recent literature on this topic highlights the significance of adding malononitrile moiety and halogen substituents to the squaraine scaffold to create redshifted fluorophores into the near-infrared optical region. Herein, a redshifted hydrophobic squaraine dye is synthesized via a three-step pathway. The reported dye is characterized by spectroscopic techniques, such as ^{1}H NMR, ^{19}F NMR, ^{13}C NMR, and high-resolution mass spectroscopy. Optical properties are also reported using absorbance and fluorescence studies. The hydrophobicity of the dye was studied with absorbance and fluorescence spectroscopy in water–methanol mixtures and showed J-aggregates as the water concentration increased. Density functional theory calculations were conducted to assess its electron delocalization as well as observe the three-dimensional geometry of the dye as a result of the dicyanomethylene modification and the two bulky phenyl groups.

Keywords: hydrophobicity; squaraine; near-infrared; fluorescence; fluorine; dicyanomethylene

1. Introduction

Near-infrared squaraine dyes are further being analyzed for their applications as fluorophores being applied to the field of bioimaging [1–5]. Squaraine dyes have been known for having a high molar absorptivity and quantum yield, which is crucial for bright near-infrared fluorophores, but poor/medium stability has been reported as the most notable drawback of squaraine dyes [6]. This poor stability is attributed to the photo-isomerization between *cis* and *trans* configurations that squaraine fluorophores typically undergo [7]. For this reason, it is critical to consider exploring different substituents on the squaraine scaffold to improve its capabilities as a fluorescent agent. It has been reported that the addition of dicyanomethylene to the central squarate has reported increased wavelength absorbance maxima compared to the typical squaraine scaffold [1,8–11]. The addition of this moiety causes a locked *cis* configuration of the dye resulting in an improvement in the dye's stability. The introduction of halogens to the squaraine scaffold has redshifted fluorophores, which is a significant optical effect when determining contrast agents for bioimaging in the NIR region [4,12–15]. To further redshift squaraine dyes, researchers have been modifying the squaraine core with different moieties to observe the optical effects of the given changes.

Along with the chemical properties described, researchers are considering the different types of applications that squaraine dyes have the potential for based on their substituents [14]. It is essential to consider the different optical effects that can be seen by
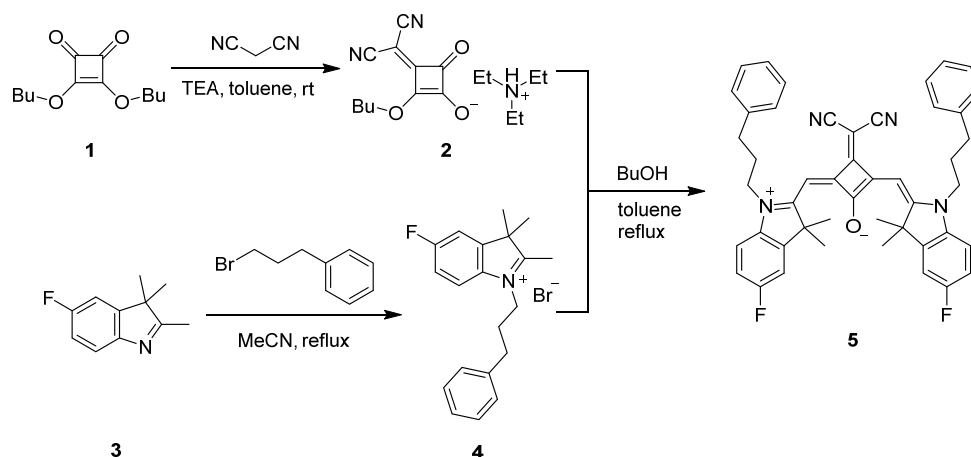
introducing hydrophobic substituents added to the squaraine scaffold. Optical studies of hydrophobic NIR dyes have been performed to observe the blueshift in dyes placed in a polar solvent [16]. However, the introduction of certain globular proteins [17,18] can combat this behavior as hydrophobic pockets of the proteins can interact with the fluorophore, improve fluorescence intensity, and demonstrate redshifts in optical data.

Herein, we report the synthesis of a fluorinated squaraine dye with a dicyanomethylene moiety in the squaraine core. The fluorine atoms are expected to improve the compound chemical property while introducing the electron-withdrawing effects experienced by known halogenated dyes [13,15,19]. The phenylpropyl groups will retain the hydrophobicity [16,20] of the fluorophore, and the dicyanomethylene will generate some chemical stability.

2. Results and Discussion

2.1. Synthesis

The synthesis of dye **5** is achieved through a three-step pathway detailed in Scheme 1. This pathway begins with the synthesis of the modified squaraine linker **2** accomplished from the reaction of substituted linker **1** with malononitrile under basic conditions in toluene for 1 h, as reported by the Würthner group [12]. In another step, fluorinated heterocycle **3** reacts with (3-bromopropyl) benzene in reflux overnight to produce heterocyclic salt **4** [15]. Compound **4** then reacts with squaraine linker **2** in the last step to generate final product **5** in good yield [6]. After the successful synthesis of dye **5**, the purity of the compound was studied with ^{1}H, ^{13}C, and ^{19}F spectra and high-resolution mass spectrometry (Figures S1–S4, Supplementary Materials).

Scheme 1. Synthetic preparation of squaraine dye **5**.

The chemical structure of compound **5**, as seen in Scheme 1, was designed with rotatable phenylpropyl groups, fluorine atoms, and dicyanomethylene. The dicyanomethylene introduced to the squaraine core exhibits a significant bathochromic shift for this scaffold compared to standard squaraine dyes. The fluorine atoms act as electron-withdrawing groups to further improve the chemical properties without significantly affecting the overall size of the compound. The phenylpropyl groups increase the number of rotatable bonds and increase the hydrophobicity of the compound.

2.2. Physicochemical Properties of Dye **5** Compared to Commercially Available Squaraine (**SQ**)

The photophysical properties for the synthesized dye **5** and general squaraine (**SQ**) were calculated using ChemAxon (MarvinSketch calculator plugin), as seen in Table 1. The logD at pH 7.4 for dye **5** was reported to be 7.31. The polarizability of dye **5** was calculated to be 79.59. The dipole moment of dye **5** was determined to be 15.34 debye compared to **SQ** reporting 9.77 debye. Dye **5** contains 10 rotatable bonds compared to standard **SQ**

that contains two; this difference is due to the introduction of phenylpropyl groups to the scaffold. The molecular volume (MV), weight (MW), and surface area (MSA) for dye **5** are 654.11, 716.88, and 1001.06, respectively. These three values are greater than the values reported for **SQ** (Figure S5), likely due to the phenylpropyl groups and fluorine atoms introduced to the scaffold.

Table 1. Physicochemical properties of dye **5** calculated using ChemAxon.

Dye	LogD (pH 7.4)	Polarizability	Dipole Moment (Debye)	Rotatable Bonds	MV ($Å^3$)	MW (g/mol)	MSA ($Å^3$)
SQ	2.96	49.01	9.77	2	394.21	424.54	613.90
5	7.31	79.59	15.34	10	654.11	716.88	1001.06

2.3. Optical Properties of Dye **5**

The absorbance spectrum of squaraine **5** was obtained at different concentrations of dye, as shown in Figure 1a. The absorbance maxima were determined to be at wavelength 670 nm. The absorbance values were plotted against the concentration of the dye to determine the molar absorptivity using the Beer–Lambert Law (Figure 1b). The same analytical procedure was used to determine the absorbance wavelength maxima and molar absorptivities of dye **5** in various solvents. The absorbance maxima are presented in Table 2, and corresponding absorbance graphs are shown in Figures S6–S9. The wavelength of the fluorescence maximum was determined for dye **5** (0.1 mM) in different solvents. These values were used to calculate Stokes shifts at each solvent.
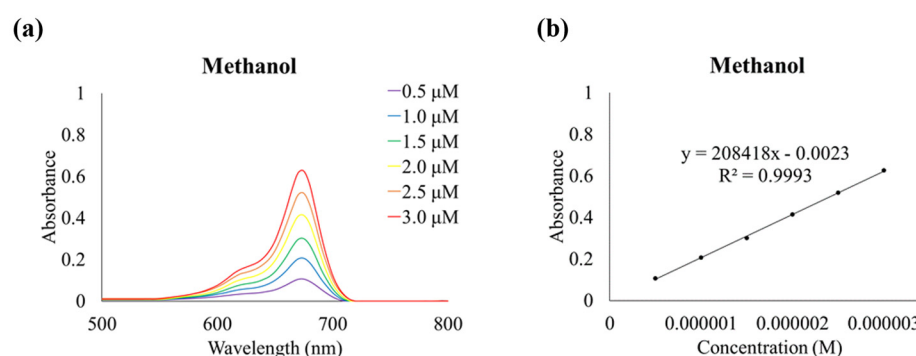

Figure 1. (**a**) The absorbance spectra of compound **5** in methanol at different concentrations (0.5, 1.0, 1.5, 2.0, 2.5, and 3.0 µM). (**b**) Linear curve demonstrating Beer–Lambert Law used to determine molar absorptivity of compound **5** as $\varepsilon = 208{,}000$ M^{-1} cm^{-1}.

Table 2. Optical properties of compound **5**.

Solvent	λ_{abs} (nm)	λ_{em} (nm)	Stokes Shift (nm)	ε (L mol^{-1} cm^{-1})	ΦF (%)
Methanol	675	691	16	208,000	25
Ethanol	675	693	18	188,000	52
Acetonitrile	675	691	16	235,000	12
Toluene	700	714	14	222,000	63
DMSO	680	698	18	188,000	34
Rhodamine800 [5]	682	700	18	113,000	25

The absorption maxima of dye **5** were studied in five different solvents. Figure 2 is a compilation of the absorbance spectra of dye **5** in all five reported solvents. The data demonstrate that the absorbance maxima in the polar solvents (MeOH, EtOH, and MeCN) remained at 675 nm, while a small 5 nm shift was observed for the absorbance maximum in DMSO. The data indicate a redshift in the absorbance maxima when observed in the

nonpolar solvent toluene by about 25 nm compared to the polar solvents. A similar trend was observed for the fluorescence wavelength maxima; solvents MeOH, EtOH, and MeCN observed maxima at 691–693 nm. The DMSO fluorescence maximum was observed at 698 nm, and the nonpolar solvent toluene observed the most significant redshift at 714 nm. These data indicate that the fluorophore is influenced by the polarity of the solvent it is exposed to, indicating fluorophore stability in nonpolar solvents.
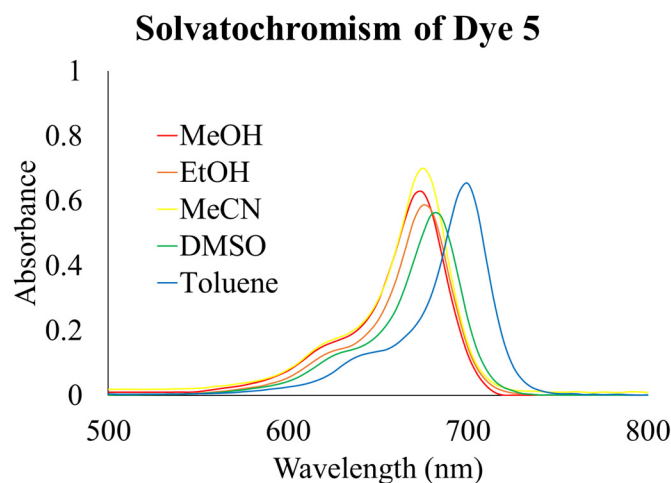

Figure 2. Solvatochromism of compound **5** (3 μM) in five different solvents: Methanol (MeOH), Ethanol (EtOH), Acetonitrile (MeCN), Dimethyl Sulfoxide (DMSO), and Toluene.

Table 2 also exemplifies the molar absorptivity of dye **5** in the different solvents and quantum yields, two significant properties that contribute to a compound's molecular brightness [20]. It is noted that molar absorptivities of 235,000 L mol^{-1} cm^{-1} and 222,000 L mol^{-1} cm^{-1} were noticed in MeCN and toluene, respectively. The highest quantum yield (63%) was analyzed from the measurements obtained from toluene. This result indicates that dye **5** has the most optimal optical properties in toluene, thus indicating a favorability for hydrophobic solvents for the highest molecular brightness.

Solvatochromism of Dye **5**

The absorbance wavelength maxima of a dye are affected by the solvent polarity, and this property is known as solvatochromism [21]. The absorbance maxima can shift, or the intensity may decrease according to the solvent's polarity. Solvatochromism is an important feature of organic molecules because it gives information about the polarity of the molecule and helps researchers to predict the potential applications [22]. The solvatochromism of dye **5** in five different solvents is presented in Figure 2. The absorbance maximum is approximately 675 nm in methanol, ethanol, acetonitrile, and dimethylsulfoxide (DMSO), and there is a 5 nm redshift in DMSO. However, absorbance maximum of dye **5** in toluene is 700 nm, showing a 25 nm redshift compared to the other four solvents.

The fluorescence intensities for dye **5** and squaraine standard **SQ** in methanol were obtained. The fluorescence intensity of the two dyes at the same concentration can be observed in Figure 3. This figure shows the significant difference in the fluorescence maxima of the two dyes where dye **5** is significantly more intense. We also see a 55 nm difference in the wavelength maxima between the two peaks, demonstrating the bathochromic shift exhibited by the introduction of dicyanomethylene modification.
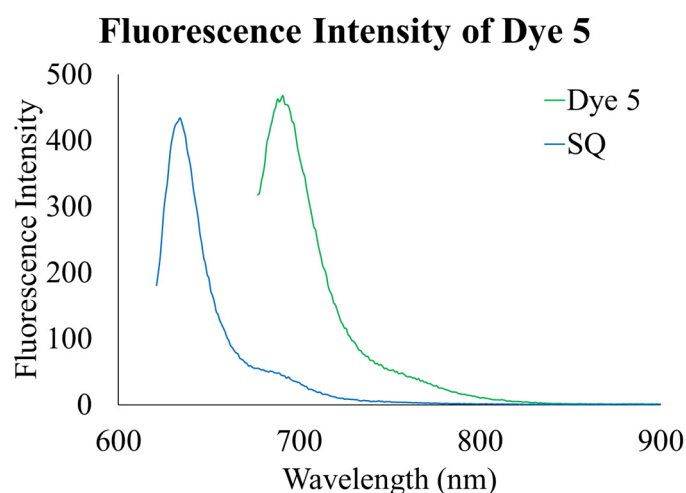
Fluorescence Intensity of Dye 5

Figure 3. Fluorescence intensity of dye **5** (0.0125 μM) compared to **SQ** (0.0125 μM) in methanol.

The hydrophobic behavior of dye **5** is observed in Figure 4. The figure indicates the absorbance spectra of the fluorophore in methanol and observes the change in absorption maxima with increasing proportions of water. It is seen that at 0 to 30% water, the absorbance spectra mostly retain their shape, demonstrating a strong monomeric signal. The intensity of the shape begins to diminish between 10 and 30% somewhat gradually. In the 40% water solution, the spectrum shows a clear formation of J-aggregates while still showing the monomer band (M). From 50 to 100%, only the dimer band (D) is shown, indicating the aggregation of the dye due to its hydrophobicity.
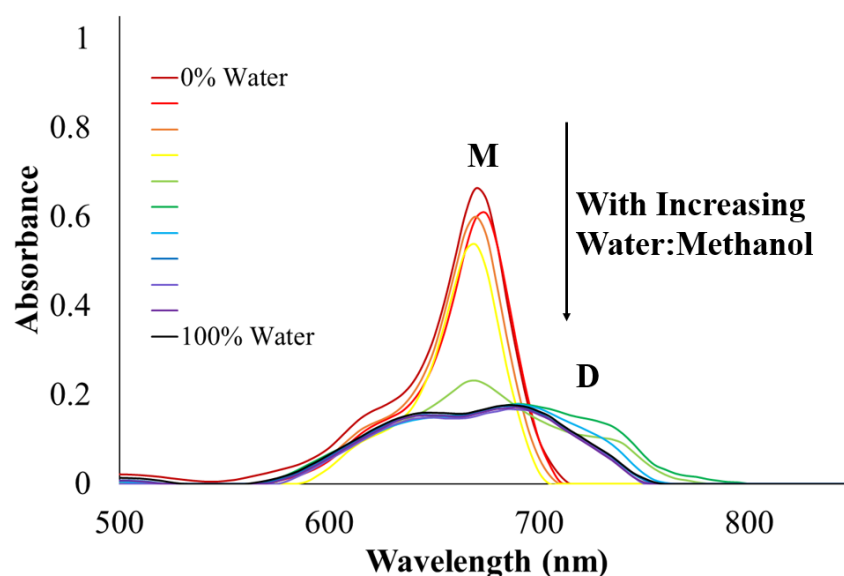
Absorbance Hydrophobicity Study

Figure 4. Absorbance spectra of compound **5** (3 μM) in increasing percentages of water (0, 10, 20, 30, 40, 50, 60, 70, 80, 90, and 100%) show a high degree of dimerization and formation of J-aggregates.

The effect of aggregation can also be visualized by observing the fluorescence intensity in increasing concentrations of water. This decrease in fluorescence intensity as presented in Figure 5, is seen through self-quenching upon dimerization of the fluorophore in the solution. The formation of the nonfluorescent aggregate corresponds to the decrease in fluorescence intensity and the slight blueshift being observed at increasing amounts of water. The fluorescence intensity gradually decreases between 0 and 30%, similar to the

behavior observed in Figure 4. At 40% water, we see the signal shape indicating a mix of monomeric and dimeric forms of the fluorophore, and then after 50% water, we see mostly the dimerization mostly diminishing the fluorescence signal.
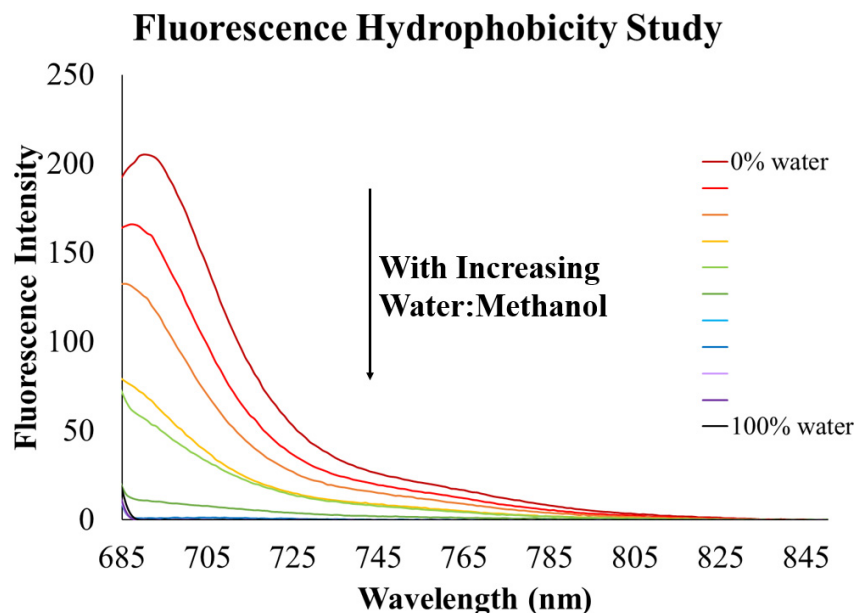

Figure 5. Fluorescence spectra of compound **5** (0.005 µM) in increasing percentages of water (0, 10, 20, 30, 40, 50, 60, 70, 80, 90, and 100%).

2.4. Density Functional Theory Calculations of Dye **5**

Density functional theory (DFT) calculations for dye **5** were obtained from Spartan 18 V1.4.5 software. The software was used to determine the electron distribution within the highest occupied molecular orbital (HOMO) and the lowest unoccupied molecular orbital (LUMO) of squaraine dye **5**, and it provides the optimal three-dimensional geometry of the molecule. The modeled HOMO and LUMO orbitals demonstrated in Figure 6 show electron distribution between the indole rings and the squaraine core. The chemical structure of symmetrical dye **5** is shown in Scheme 1, demonstrating two fluorine atoms on the indolium rings and two phenylpropyl groups appended to the nitrogen atom of the heterocycle. The two heterocycles are joined together by a conjugated cyclobutene ring containing a dicyanomethylene group. These features are shown in the optimized molecular geometry seen in Figure 6. The HOMO energy level is shown to be −5.26 eV, and the LUMO energy level was determined to be −3.33 eV. The dicyanomethylene, the negatively charged oxygen, and the heterocycle containing uncharged nitrogen contribute to the HOMO energy level. The LUMO energy level shows electron distribution across the opposite heterocycle containing positively charged nitrogen and the carbons of the cyclobutene bound to the heterocycles. The difference between the two energy levels was calculated to be 1.93 eV as an energy gap. The figure shows electron delocalization occurring across the conjugated system of the dye, excluding the phenylpropyl groups because these are separated from the conjugated system by three sp^3 carbons.

The software was also used to visualize the optimal molecular geometry of the compound. In Figure 6, one can observe the twist in geometry associated with the bulky substituents facing away from the dicyanomethylene group. This twist in the geometry resembles the configuration observed for other squaraines containing this dicyanomethylene modification that is not observed in unmodified squaraines. This twist in structure geometry demonstrates the optimal three-dimensional geometry of the compound with all its bulky groups. The introduction of the dicyanomethylene modification introduces a rigidity of the squaraine conformation, thus adding a level of chemical stabilty to the compound not observed in typical squaraines.
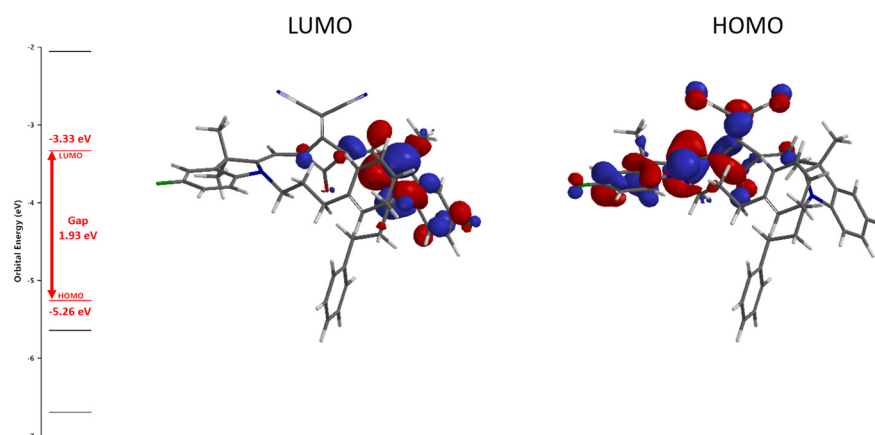
Figure 6. Theoretical calculations of HOMO/LUMO energy levels of compound **5** were obtained from Spartan 18 V1.4.5 software (Wavefunction, Inc., Irvine, CA, USA). DFT calculation was achieved at the B3LYP/6-311G level.

3. Materials and Methods

3.1. Materials

The reagents and solvents shown in Scheme 1 were obtained from Combi-Blocks (San Diego, CA, USA), Alfa Aesar (Ward Hill, MA, USA), and Sigma Aldrich (St. Louis, MO, USA). Reaction progress was monitored through thin-layer chromatography utilizing glass-backed 250 μm Silica XHL TLC Plates w/UV254 from Sorbent Technologies (Norcross, GA, USA) with 5% methanol in a dichloromethane mobile phase solvent system. Compounds were purified using flash column chromatography using 63–200 μm, 60A silica gel from Sorbent Technologies (Norcross, GA, USA). Characterization of compounds was accomplished using ^{1}H NMR and ^{19}F NMR obtained from 400 MHz Bruker Avance Spectrometer from Bruker Corporation (Billerica, MA, USA). NMR samples were prepared using NMR solvents obtained from Cambridge Isotope Laboratories (Andover, MA, USA). HRMS was obtained from the Georgia State University Mass Spectrometry Facility using Waters Q-TOF micro (ESI-Q-TOF) mass spectrometer (Waters Corporation, Milford, MA, USA).

3.2. Synthesis

Synthesis of triethylammonium 2-butoxy-3-(dicyanomethylene)-4-oxocyclobut-1-en-1-plate (**2**) is reported in the literature by the Würthner group [12].

Synthesis of 5-fluoro-2,3,3-trimethyl-1-(3-phenylpropyl)-3*H*-indol-1-ium bromide (**4**). This compound is reported in the literature by the Henary group [20].

Synthesis of (Z)-3-(dicyanomethylene)-4-((5-fluoro-3,3-dimethyl-1-(3-phenylpropyl)-3*H*-indol-1-ium-2-yl) methylene)-2-(((E)-5-fluoro-3,3-dimethyl-1-(3-phenylpropyl)indolin-2-ylidene) methyl) cyclobut-1-en-1-olate (**5**): In a 50-mL round-bottom flask, fluorinated indolium salt **4** (2 mol eq) reacted with squaraine linker **2** (1 mol eq) in a butanol/toluene solvent mixture overnight under reflux. The reaction mixture was then dried under vacuum to remove solvent mixture. The crude product was purified using alumina flash column chromatography, 0–5% methanol/dichloromethane solvent system. Final compound was obtained in 52% yield. MP: 192–194 °C; ^{1}H NMR (400 MHz, CDCl$_3$) δ1.75 (s, 6H), 2.14 (d, *J* = 7.2 Hz, 2H), 2.80 (t, *J* = 11.3 Hz, 2H), 4.00 (t, *J* = 16.0 Hz, 2H), 6.55 (s, 1H), 6.70 (m, 1H), 6.90 (m, 1H), 7.00 (m, 1H), 7.20 (m, 3H), 7.55 (m, 2H). ^{19}F NMR (400 MHz, DMSO-d_6) $\delta-$117.62. [13]C NMR (100 MHz, CDCl$_3$) δ 26.6, 28.8, 32.7, 40.9, 43.9, 49.6, 49.6, 89.3, 110.2, 110.5, 110.6, 110.7, 114.6, 114. 119.01, 126.3, 128.5, 128.6, 137.8, 140.6, 144.2, 144.3, 159.3, 161.8, 166.7, 167.7, 171.6, 172.9. High-resolution mass spectrum [M]$^+$ calculated for [C$_{47}$H$_{42}$F$_2$N$_4$O]$^+$ 716.3327; found 716.2811.

3.3. Analytical Instrumentation

Absorbance spectra for squaraine dye **5** were obtained using Varian Cary 50 Spectrophotometer (Agilent Technologies, Santa Clara, CA, USA). This instrument was interfaced to a PC with spectral bandwidth of 2 nm. Fluorescence spectra for squaraine dye **5** were obtained using Shimadzu RF-1501 Spectrofluorometer (Shimadzu Instruments, Columbia, MD, USA) interfaced to a PC with spectral bandwidth set to 10 nm and sensitivity set to a high setting. Absorbance and fluorescence cuvettes (Sigma Aldrich, St. Louis, MO, USA) with a path length of 1.00 cm were used, and all calculations were performed using Microsoft Excel 2019 (Microsoft Corporation, Redmond, WA, USA).

3.4. Analytical Instrumentation

Squaraine dye **5** samples were weighed on an analytical balance (5-digit) into amber glass vials from Fischer Scientific (Pittsburg, PA, USA). A 1 mM solution of dye **5** was made in dimethyl sulfoxide. The vial was capped and sonicated for 20 min.

3.5. Determination of Molar Absorptivity

The 1 mM stock solutions of dye **5** were diluted into different concentrations (0.5 μM, 1.0 μM, 1.5 μM, 2.0 μM, 2.5 μM, and 3.0 μM) in methanol. The most concentrated sample demonstrated an absorbance value of less than one, and the absorbance maximum (wavelength) in nanometers was recorded. Absorbance values at that wavelength were recorded for the different concentrations and were plotted against the corresponding concentrations in Microsoft Excel to determine molar absorptivity from the linear slope.

3.6. Optical Hydrophobicity Studies

Several 5 mL solvent samples containing various percentages of water were prepared (0, 10, 20, 30, 40, 50, 60, 70, 80, 90, and 100% water). A corresponding blank (baseline) was measured before the samples at different percentages of water were measured. For each sample, 10 μL of the 1 mM stock solution was diluted into the corresponding solvent samples (3 μM solution), and absorbance spectra were observed. The data from absorbance spectra were plotted on Microsoft Excel as absorbance versus wavelength to observe absorbance changes based on the percentage of water in the solvent. Similarly, the stock solution was used to prepare 0.005 μM samples of dye in corresponding solvent samples to measure fluorescence intensity versus wavelength as a result of an increasing percentage of water.

3.7. Physicochemical Studies

Spartan 18 V1.4.5 software (Wavefunction Inc., Irvine, CA, USA) was used to generate DFT calculations at the B3LYP level and a 6-311+G**. HOMO/LUMO energy levels and optimized geometries were generated. ChemAxon MarvinSketch (Budapest, Hungary) was used to calculate LogD at pH 7.4, polarizability, dipole moment, rotatable bonds, molecular volume, molecular weight, and molecular surface area for both compound **5** and standard squaraine (**SQ**).

4. Conclusions

In this study, we reported the synthesis of a fluorine-containing squaraine dye with a dicyanomethylene moiety in the squaraine core. The fluorine atom and the propyl phenyl group on the compound introduce hydrophobicity to the structure. The dye shows λ_{max} between 675–700 nm in various solvents, and the largest redshift is observed in toluene due to the hydrophobicity of the compound. The molar extinction coefficients range from 188,000 to 235,000 M^{-1} cm^{-1}. The hydrophobic behavior of the dye was studied in methanol with the addition of an increasing water ratio. The sharp monomeric peak of the dye disappears after 30% water addition and forms the J-aggregate peaks. As the dye aggregates with increasing water proportions, the fluorescence also diminishes. While the electron density is on the dicyano moiety and the heterocycle containing uncharged

nitrogen, the electron density on LUMO was located on the positively charged nitrogen heterocycle. The difference between the HOMO and LUMO levels was calculated as 1.93 eV.

References

1. Ilina, K.; MacCuaig, W.M.; Laramie, M.; Jeouty, J.N.; McNally, L.R.; Henary, M. Squaraine Dyes: Molecular Design for Different Applications and Remaining Challenges. *Bioconjugate Chem.* **2020**, *31*, 194–213. [CrossRef]
2. Yao, D.; Wang, Y.; Zou, R.; Bian, K.; Liu, P.; Shen, S.; Yang, W.; Zhang, B.; Wang, D. Molecular Engineered Squaraine Nanoprobe for NIR-II/Photoacoustic Imaging and Photothermal Therapy of Metastatic Breast Cancer. *ACS Appl. Mater. Interfaces* **2020**, *12*, 4276–4284. [CrossRef]
3. Sreejith, S.; Joseph, J.; Lin, M.; Menon, N.V.; Borah, P.; Ng, H.J.; Loong, Y.X.; Kang, Y.; Yu, S.W.-K.; Zhao, Y. Near-Infrared Squaraine Dye Encapsulated Micelles for in Vivo Fluorescence and Photoacoustic Bimodal Imaging. *ACS Nano* **2015**, *9*, 5695–5704. [CrossRef]
4. Serpe, L.; Ellena, S.; Barbero, N.; Foglietta, F.; Prandini, F.; Gallo, M.P.; Levi, R.; Barolo, C.; Canaparo, R.; Visentin, S. Squaraines bearing halogenated moieties as anticancer photosensitizers: Synthesis, characterization and biological evaluation. *Eur. J. Med. Chem.* **2016**, *113*, 187–197. [CrossRef]
5. Alessi, A.; Salvalaggio, M.; Ruzzon, G. Rhodamine 800 as reference substance for fluorescence quantum yield measurements in deep red emission range. *J. Lumin.* **2013**, *134*, 385–389. [CrossRef]
6. Yadav, Y.; Owens, E.; Nomura, S.; Fukuda, T.; Baek, Y.; Kashiwagi, S.; Choi, H.S.; Henary, M. Ultrabright and Serum-Stable Squaraine Dyes. *J. Med. Chem.* **2020**, *63*, 9436–9445. [CrossRef]
7. Galliano, S.; Novelli, V.; Barbero, N.; Smarra, A.; Viscardi, G.; Borrelli, R.; Sauvage, F.; Barolo, C. Dicyanovinyl and Cyano-Ester Benzoindolenine Squaraine Dyes: The Effect of the Central Functionalization on Dye-Sensitized Solar Cell Performance. *Energies* **2016**, *9*, 486. [CrossRef]
8. Wu, J.; Yang, D.; Wang, Q.; Yang, L.; Sasabe, H.; Sano, T.; Kido, J.; Lu, Z.; Huang, Y. Central dicyanomethylene-substituted unsymmetrical squaraines and their application in organic solar cells. *J. Mater. Chem. A* **2018**, *6*, 5797–5806. [CrossRef]
9. Wei, Y.; Hu, X.; Shen, L.; Jin, B.; Liu, X.; Tan, W.; Shangguan, D. Dicyanomethylene Substituted Benzothiazole Squaraines: The Efficiency of Photodynamic Therapy In Vitro and In Vivo. *EBioMedicine* **2017**, *23*, 25–33. [CrossRef]
10. dos Santos Pisoni, D.; Petzhold, C.L.; de Abreu, M.P.; Rodembusch, F.S.; Campo, L.F. Synthesis, spectroscopic characterization and photophysical study of dicyanomethylene-substituted squaraine dyes. *Comptes Rendus Chim.* **2012**, *15*, 454–462. [CrossRef]
11. Qin, C.; Numata, Y.; Zhang, S.; Yang, X.; Islam, A.; Zhang, K.; Chen, H.; Han, L. Novel Near-Infrared Squaraine Sensitizers for Stable and Efficient Dye-Sensitized Solar Cells. *Adv. Funct. Mater.* **2014**, *24*, 3059–3066. [CrossRef]
12. Mayerhöffer, U.; Fimmel, B.; Würthner, F. Bright Near-Infrared Fluorophores Based on Squaraines by Unexpected Halogen Effects. *Angew. Chem. Int. Ed.* **2012**, *51*, 164–167. [CrossRef] [PubMed]
13. Casa, S.; Henary, M. Synthesis and Applications of Selected Fluorine-Containing Fluorophores. *Molecules* **2021**, *26*, 1160. [CrossRef] [PubMed]
14. Barcenas, G.; Biaggne, A.; Mass, O.A.; Wilson, C.K.; Obukhova, O.M.; Kolosova, O.S.; Tatarets, A.L.; Terpetschnig, E.; Pensack, R.D.; Lee, J.; et al. First-principles studies of substituent effects on squaraine dyes. *RSC Adv.* **2021**, *11*, 19029–19040. [CrossRef]
15. Owens, E.A.; Hyun, H.; Dost, T.L.; Lee, J.H.; Park, G.; Pham, D.H.; Park, M.H.; Choi, H.S.; Henary, M. Near-Infrared Illumination of Native Tissues for Image-Guided Surgery. *J. Med. Chem.* **2016**, *59*, 5311–5323. [CrossRef]

16. Owens, E.A.; Tawney, J.G.; Henary, M.M. 2-{(E)-2-[(3E)-2-Chloro-3-{(2E)-2-[1,1-dimethyl-3-(3-phenylpropyl)-1,3-dihydro-2H-benzo[e]indol-2-ylidene]-ethylidene}cyclohex-1-en-1-yl]ethenyl}-1,1-dimethyl-3-(3-phenylpropyl)-1H-benzo[*e*]indolium Iodide. *Molbank* **2014**, *2014*, M814. [CrossRef]

17. Aristova, D.; Volynets, G.; Chernii, S.; Losytskyy, M.; Balanda, A.; Slominskii, Y.; Mokhir, A.; Yarmoluk, S.; Kovalska, V. Far-red pentamethine cyanine dyes as fluorescent probes for the detection of serum albumins. *R Soc. Open Sci.* **2020**, *7*, 200453. [CrossRef]

18. Levitz, A.; Marmarchi, F.; Henary, M. Synthesis and Optical Properties of Near-Infrared meso-Phenyl-Substituted Symmetric Heptamethine Cyanine Dyes. *Molecules* **2018**, *23*, 226. [CrossRef]

19. Biffinger, J.C.; Kim, H.W.; DiMagno, S.G. The Polar Hydrophobicity of Fluorinated Compounds. *ChemBioChem* **2004**, *5*, 622–627. [CrossRef]

20. Buabeng, E.R.; Henary, M. 2-((E)-2-((E)-4-Chloro-5-(2-((E)-5-methoxy-3,3-dimethyl-1-(3-phenylpropyl)indolin-2-ylidene) ethylidene)-1,1-dimethyl-1,2,5,6-tetrahydropyridin-1-ium-3-yl)vinyl)-5-methoxy-3,3-dimethyl-1-(3-phenylpropyl)-3H-indol-1-ium. *Molbank* **2021**, *2021*, M1270. [CrossRef]

21. Essam, Z.M.; Ozmen, G.E.; Setiawan, D.; Hamid, R.R.; Abd El-Aal, R.M.; Aneja, R.; Hamelberg, D.; Henary, M. Donor acceptor fluorophores: Synthesis, optical properties, TD-DFT and cytotoxicity studies. *Org. Biomol. Chem.* **2021**, *19*, 1835–1846. [CrossRef] [PubMed]

22. Nigam, S.; Rutan, S. Principles and Applications of Solvatochromism. *Appl. Spectrosc.* **2001**, *55*, 362A–370A. [CrossRef]